Available online at www.sciencedirect.com
SCIENCE DIRECT®
International Journal of Heat and Mass Transfer 48 (2005) 779–792
International Journal of HEAT and MASS TRANSFER
www.elsevier.com/locate/ijhmt

Laminar natural convection in a vertical stack of parallelogrammic partial enclosures with variable geometry

V.A.F. Costa [a,*], M.S.A. Oliveira [a], A.C.M. Sousa [a,b]

[a] Departamento de Engenharia Mecânica, Universidade de Aveiro, Campus Universitário de Santiago, 3810-193 Aveiro, Portugal
[b] Department of Mechanical Engineering, University of New Brunswick, Fredericton, NB, Canada E3B5A3

Received 7 July 2003
Available online 6 November 2004

Abstract

A numerical study is conducted for laminar natural convection heat transfer occurring in a vertical stack of parallelogrammic partial enclosures. The partitions separating adjacent enclosures are always parallel to each other, however their angle relative to the horizontal can change. The length of each partition is less than the width of the main enclosure, which has an aspect ratio of 5. Adjacent enclosures are thermally linked through the fluid exchange, and through the finite thermal conductivity of the partitions. The thermal diode effect offered by the geometry is analyzed in terms of the partitions' inclination angle and materials for different thermal boundary conditions/operating conditions. The thermal diode effect, and even its actuating direction, can be changed by changing the inclination angle of the partitions. The main focus of the present work deals with the heat transfer analysis based on the overall Nusselt number, and the visualization of the flow field and heat transfer mechanisms, by using the isotherms, the streamlines and the heatlines. Results clearly indicate the high potential of this configuration, based on the thermal diode effect, to be used as an effective heat transfer device in real situations of thermal engineering. The number of governing parameters is high, and the results are presented only for situations selected on the basis of their relevance. For computational expediency, it is analyzed the solution obtained for one single parallelogrammic partial enclosure of the stack, which is thermally linked with its adjacent enclosures by using vertical cyclic boundary conditions. This procedure has some potential, since it yields results with good accuracy to predict the overall thermal behavior of the stack.

1. Introduction

Natural convection in enclosures of rectangular and square cross-section has been extensively studied, and the literature is vast on this subject, both when the enclosures are filled with a single fluid or filled with a fluid saturated porous medium. An excellent overview of such body of work can be found in [1,2]. The search for efficient thermal systems has led to different strategies, which include, among others, fins attached to the active enclosure walls [3–6], partitioned enclosures [7–12], enclosures with triangular cross-sections [13–15] or with trapezoidal cross-sections [16,17].

* Corresponding author. Tel.: +351 234 370 829; fax: +351 234 370 953.
E-mail address: v_costa@mec.ua.pt (V.A.F. Costa).

0017-9310/$ - see front matter © 2004 Elsevier Ltd. All rights reserved.
doi:10.1016/j.ijheatmasstransfer.2004.09.012

Nomenclature

g	gravitational acceleration
H	height
H	heatfunction
k	thermal conductivity
L	length
n	outward normal
Nu	Nusselt number
p	pressure
Pr	Prandtl number
Ra	Rayleigh number
R_c	thermal conductivity ratio, k_s/k_f
T	temperature
u, v	Cartesian velocity components
x, y	Cartesian co-ordinates

Greek symbols

α	thermal diffusivity
β	volumetric expansion coefficient
δ	elementary gap width
Δ	shutters' thickness
θ	inclination angle
v	kinematic viscosity
ρ	density
ψ	streamfunction

Subscripts

f	fluid
H	higher value
L	lower value
s	shutter
*	dimensionless

In what concerns natural convection heat transfer in parallelogrammic enclosures, there is a limited number of studies, and they highlight the strong potential of this geometry to be used in efficient heat transfer systems [18–23]. Two of these studies consider separating walls of finite thermal conductivity in a vertical stack of parallelogrammic enclosures [18,21]. Parallelogrammic enclosures are characterized by behaving as thermal diodes, which, depending on the inclination angle of the separating walls, may yield very different thermal performances [18,20,21]. The overall Nusselt number for the parallelogrammic enclosure can be several times higher (or lower) than that for the corresponding rectangular or square enclosures. It should be mentioned that similar configurations in the form of venetian blind systems have been already analyzed [24–26], however their purpose and operating conditions are different from those of the vertical stacks proposed in the present work.

The thermal performance of the parallelogrammic enclosures is dependent, among others, of the inclination angle and of the aspect ratio of the enclosure. However, due to constructive reasons, their geometry is usually fixed. Therefore, it is not possible to change their thermal performance by changing their geometry, and in particular the inclination angle. In this work it is proposed an arrangement of parallelogrammic partial enclosures, in the form of a vertical stack, in such a way that the geometry can be changed by changing the inclination angle of the partitions. In this case, each parallelogrammic enclosure is not fully closed, and exchanges fluid with its neighboring enclosures in the stack. The gap for fluid exchange increases as increases the inclination angle. The adjacent parallelogrammic enclosures in the stack are thus thermally connected through the fluid exchange and through the separating walls of finite thermal conductivity. The thermal performance of the stack can be optimized for specified thermal boundary conditions by varying the inclination angle. This system, which, as already stated, behaves as a thermal diode, finds many applications, such as, for example, walls of variable thermal characteristics, and even walls whose thermal performance can be adjusted to the desired direction of the heat transfer.

From the heat and mass transfer viewpoint, this is a problem full of interesting phenomenological features. Taken globally, it is a natural convection problem but, taken from a particular partial enclosure, it is a mixed convection problem, where the incoming flow has a velocity imposed by the natural convection occurring in the global system. From the numerical viewpoint, it is also a very interesting problem, for which it is tempting to use cyclic boundary conditions.

In this study, the thermal performance of the system is analyzed for some selected combinations of the dimensionless governing parameters, and the flow field and heat transfer are visualized through the use of the isotherms, streamlines and heatlines [27]. For this purpose it is used a vertical stack with four equally spaced partitions (shutters), thus forming five contiguous enclosures. Special attention is given to the mid-height enclosure. Due to constructive reasons, the top and bottom enclosures in the stack are not parallelogrammic enclosures, but trapezoidal enclosures, as the stack is contained in a rectangular cross-section cavity. For a vertical stack with a large number of parallelogrammic partial enclosures, it is analyzed the viability of calculating the natu-

ral convection problem for a single enclosure only, which is linked to its adjacent enclosures through vertical cyclic boundary conditions.

Results clearly show the strong engineering potential of the proposed vertical stack arrangement, with the possibility of geometry variation. A finding of particular interest is to realize that the overall thermal performance of the stack can be analyzed on the basis of single parallelogrammic enclosures with imposed cyclic spatial boundary conditions along the vertical direction of the stack.

2. Physical and numerical modeling

2.1. Physical model and assumptions

The domain under analysis is, as sketched in Fig. 1, a two-dimensional vertical stack of parallelogrammic partial enclosures. The stack has height H, and the shutters are of rectangular cross-section, with length $L - 2\delta$, and thickness Δ. They form an angle θ relative to the horizontal direction. The inclination angle θ can be changed, in order to obtain different thermal performances of the vertical stack. As the inclination angle changes so changes the gap between the vertical walls of the stack and the shutters, thus forming open parallelogrammic enclosures, referred to as partial enclosures. When the shutters assume the horizontal position ($\theta = 0$), each existing lateral gap has the minimum width δ, as the shutter length is $L - 2\delta$. For a given inclination angle θ, the minimum gap width is obtained as $H\{(1/2)L_* - [(1/2)L_* - \delta_*]\cos\theta - (1/2)\Delta_*\sin\theta\}$, where the dimensions were made dimensionless using the height H. Each partial enclosure, exception made to the top and bottom trapezoidal enclosures of the stack, has a height, measured at $x = L/2$, of $H[(1 - 4\Delta_*)/5 - \Delta_*(1/\cos\theta - 1)]$.

The vertical walls of the stack are maintained at constant different levels of temperature, and the horizontal top and bottom walls are assumed to be perfect thermal insulators. The shutters have finite thermal conductivity, thus establishing an additional thermal connection between contiguous parallelogrammic partial enclosures.

The stack is filled with a Newton–Fourier fluid, which flows under steady-state conditions, in laminar regime. This fluid is taken as incompressible but expands or contracts under temperature changes, and this effect is modeled through the Boussinesq approach. For the energy conservation analysis, it is assumed that the

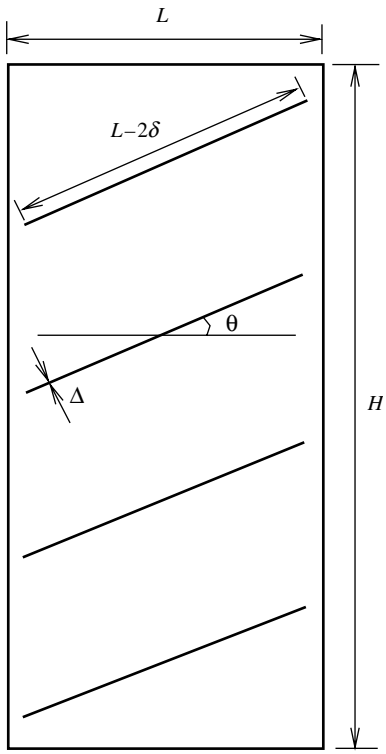

Fig. 1. Physical model and geometry.

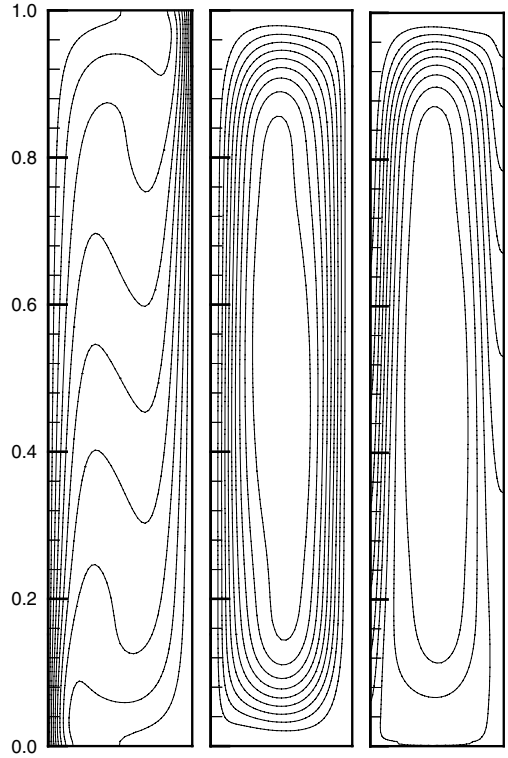

Fig. 2. Dimensionless isotherms (left), streamlines (center) and heatlines (right), for the enclosure with no shutters, $L_* = 0.2$ and $Ra = 10^7$ ($\Delta T_* = 0.10$, $\Delta\psi_* = 6.52$, $\Delta H_* = 0.50$).

thermal levels are small, resulting in negligible thermal radiation heat transfer between the walls, while the fluid is assumed to be radiatively non-participating. The energy terms due to viscous dissipation and change of temperature due to reversible deformation (work of pressure forces) are not considered.

2.2. Model equations

Taking the dimensionless variables

$$(u_*, v_*) = (u, v)/(\alpha/H) \tag{1}$$

$$(x_*, y_*) = (x, y)/H \tag{2}$$

$$T_* = (T - T_L)/(T_H - T_L) \tag{3}$$

$$p_* = (p + \rho_L g y)/\lfloor \rho_L (\alpha/H)^2 \rfloor \tag{4}$$

where p_* is the dimensionless driving pressure, the problem under analysis is governed by the following set of dimensionless partial differential equations, written in conservative form: Mass conservation:

$$\frac{\partial u_*}{\partial x_*} + \frac{\partial v_*}{\partial y_*} = 0 \tag{5}$$

Momentum:

$$\frac{\partial}{\partial x_*}(u_* u_*) + \frac{\partial}{\partial y_*}(v_* u_*) = -\frac{\partial p_*}{\partial x_*} + Pr\left(\frac{\partial^2 u_*}{\partial x_*^2} + \frac{\partial^2 u_*}{\partial y_*^2}\right) \tag{6}$$

$$\frac{\partial}{\partial x_*}(u_* v_*) + \frac{\partial}{\partial y_*}(v_* v_*) = -\frac{\partial p_*}{\partial y_*} + Pr\left(\frac{\partial^2 v_*}{\partial x_*^2} + \frac{\partial^2 v_*}{\partial y_*^2}\right) + RaPrT_* \tag{7}$$

Energy conservation, for the fluid:

$$\frac{\partial}{\partial x_*}(u_* T_*) + \frac{\partial}{\partial y_*}(v_* T_*) = \frac{\partial^2 T_*}{\partial x_*^2} + \frac{\partial^2 T_*}{\partial y_*^2} \tag{8}$$

Energy conservation, for the shutters:

$$0 = R_c\left(\frac{\partial^2 T_*}{\partial x_*^2} + \frac{\partial^2 T_*}{\partial y_*^2}\right) \tag{9}$$

The above equations introduce the following dimensionless parameters:

$$Pr = \nu/\alpha; \quad R_c = k_s/k_f \tag{10}$$

$$Ra = \frac{g\beta(T_H - T_L)H^3}{\nu\alpha} \tag{11}$$

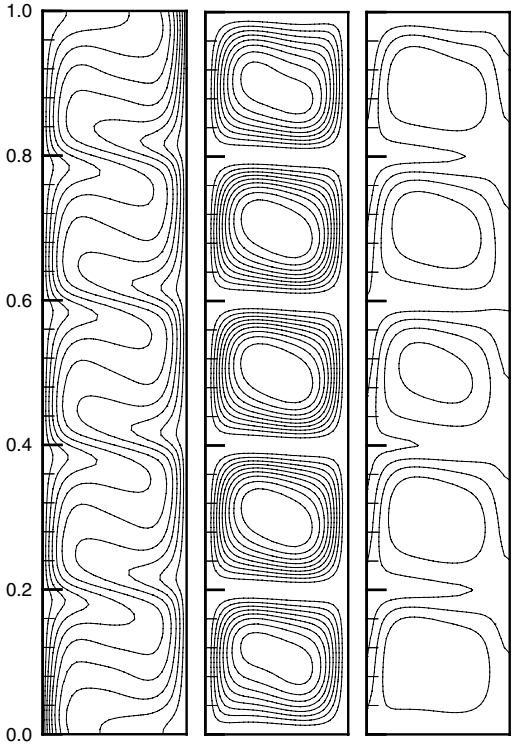

Fig. 3. Dimensionless isotherms (left), streamlines (center) and heatlines (right), for the enclosure with shutters, $\theta = 0°$, $R_c = 1$, $L_* = 0.2$ and $Ra = 10^7$ ($\Delta T_* = 0.10$, $\Delta\psi_* = 1.27$, $\Delta H_* = 0.42$).

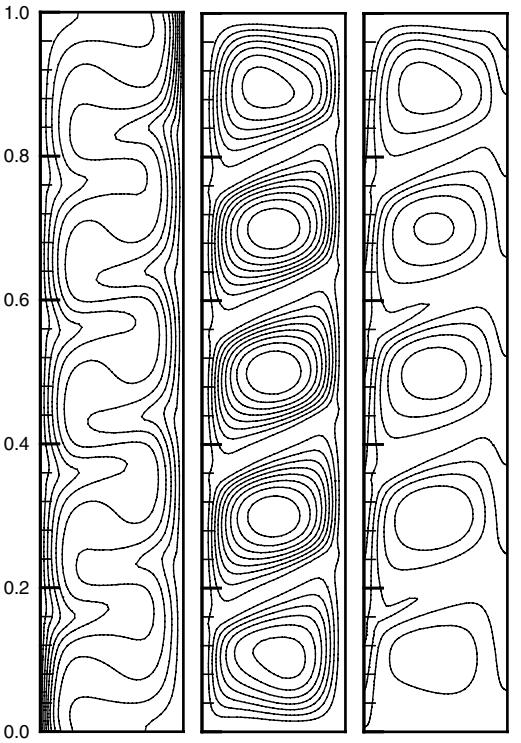

Fig. 4. Results for $\theta = 30°$, $R_c = 1$, $L_* = 0.2$ and $Ra = 10^7$ ($\Delta T_* = 0.10$, $\Delta\psi_* = 1.79$, $\Delta H_* = 0.39$). Base legend as for Fig. 3.

In addition to these dimensionless parameters, to solve the problem, the inclination angle, θ, the main enclosure aspect ratio, $L_* = L/H$, the dimensionless elementary gap width, $\delta_* = \delta/H$, and the dimensionless thickness of the shutters, $\Delta_* = \Delta/H$, need to be specified. To solve the problem it is thus necessary to specify seven dimensionless governing parameters, namely: Pr, Ra, R_c, θ, L_*, δ_* and Δ_*.

2.3. Boundary conditions

The required boundary conditions are as follows:

For the walls of the main enclosure and for the shutters

$$u_* = v_* = 0 \tag{12}$$

For the vertical walls of the main enclosure

$$T_*(0, y_*) = 1; \quad T_*(L_*, y_*) = 0 \tag{13}$$

For the fluid–shutters interfaces, to satisfy the energy balance

$$-k_s \frac{\partial T_s}{\partial n} = -k_f \frac{\partial T_f}{\partial n} \tag{14}$$

where n is the local normal of the shutter outer surface. The dimensionless version of Eq. (14) takes the form

$$(\partial T_*/\partial n_*)_f = R_c (\partial T_*/\partial n_*)_s \tag{15}$$

For adiabatic top and bottom walls of the main enclosure

$$\frac{\partial T_*}{\partial y_*} = 0 \tag{16}$$

2.4. Heat transfer

The overall heat transfer rate is determined based on the overall Nusselt number, which is defined as

$$Nu = \frac{\int_0^H -k_f \left(\frac{\partial T}{\partial x}\right)_{x=0} dy}{k_f[(T_H - T_L)/L]H} = L_* \int_0^1 \left(-\frac{\partial T_*}{\partial x_*}\right)_{x_*=0} dy_* \tag{17}$$

The top and bottom walls of the main enclosure are adiabatic, therefore the derivative $\partial T_*/\partial x_*$ in Eq. (17) can be taken either at $x_* = 0$ or at $x_* = L_*$. The denominator of Eq. (17) refers to the pure conduction situation through the stagnant fluid of thermal conductivity k_f, for the thermal gradient $(T_H - T_L)/L$.

2.5. Numerical modeling

The numerical method used in this work is a two-dimensional laminar version of the control-volume based finite element method described in [28], which is particularly well-suited to be used in domains with

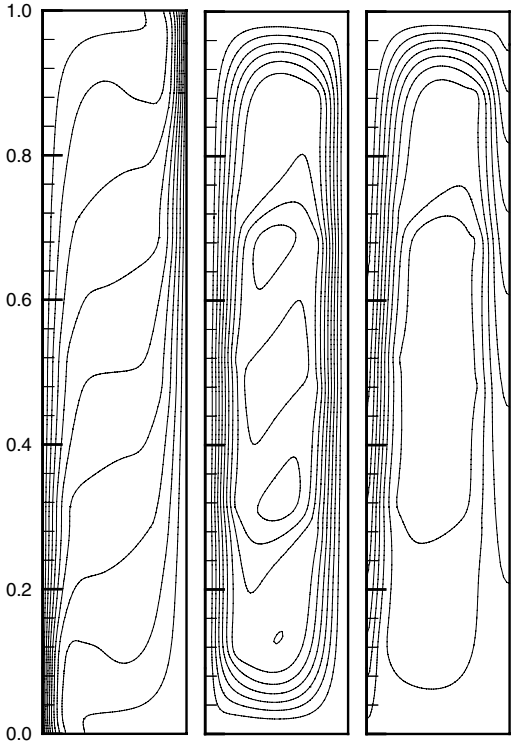

Fig. 5. Results for $\theta = 60°$, $R_c = 1$, $L_* = 0.2$ and $Ra = 10^7$ ($\Delta T_* = 0.10$, $\Delta\psi_* = 3.01$, $\Delta H_* = 0.45$). Base legend as for Fig. 3.

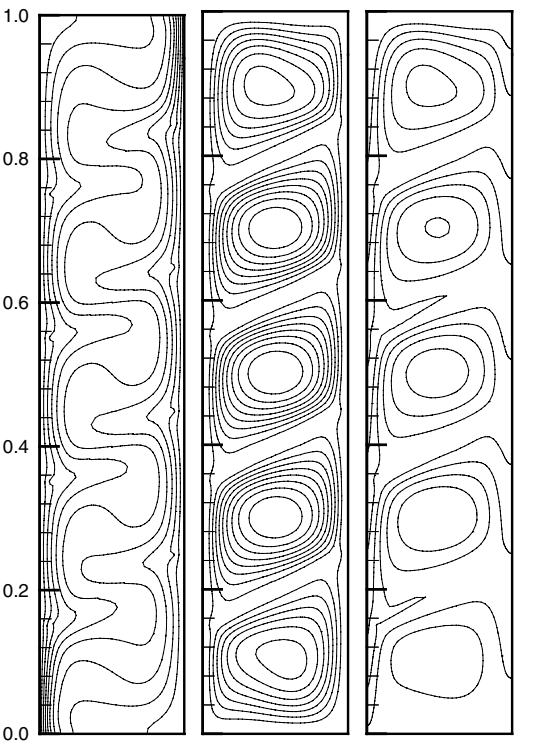

Fig. 6. Results for $\theta = 30°$, $R_c = 100$, $L_* = 0.2$ and $Ra = 10^7$ ($\Delta T_* = 0.10$, $\Delta\psi_* = 1.78$, $\Delta H_* = 0.40$). Base legend as for Fig. 3.

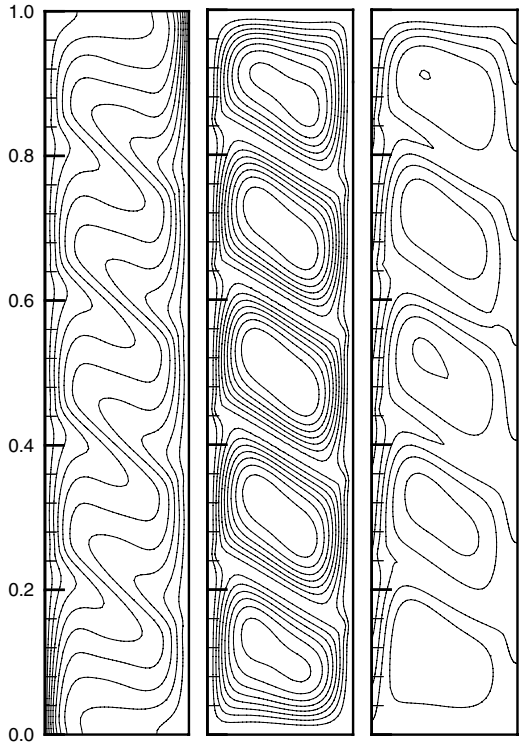

Fig. 7. Results for $\theta = -30°$, $R_c = 1$, $L_* = 0.2$ and $Ra = 10^7$ ($\Delta T_* = 0.10$, $\Delta\psi_* = 1.32$, $\Delta H_* = 0.35$). Base legend as for Fig. 3.

irregular geometries. Such numerical method has been extensively used, with good results, to solve natural convection problems in enclosures. After a few preliminary tests of the asymptotic type, the following non-uniform structured mesh was selected: 13 columns of nodes to cover the region between each main vertical wall of the stack and the shutters; two rows of nodes along each shutter; 31 columns of nodes to cover the region of the partial enclosures; and 31 rows of nodes to cover the region of each partial enclosure. This mesh results in a global non-uniform structured mesh with 55×159 nodes. The heat transfer problem is solved as a conjugate problem, the temperature field being evaluated implicitly and simultaneously in the overall domain.

3. Results and analysis

3.1. Values of the dimensionless parameters

All the reported results were obtained for a fluid of $Pr = 0.73$, and for shutters with $\delta_* = \Delta_* = 0.001$. The remaining four dimensionless parameters, Ra, R_c, θ and L_* were changed in order to analyze their influence upon the heat transfer and fluid flow results. Stream-function is made dimensionless as $\psi_* = \psi/(\rho\alpha)$, and heat-function is made dimensionless as $H_* = L_* H/[k_f(T_H - T_L)]$ [27].

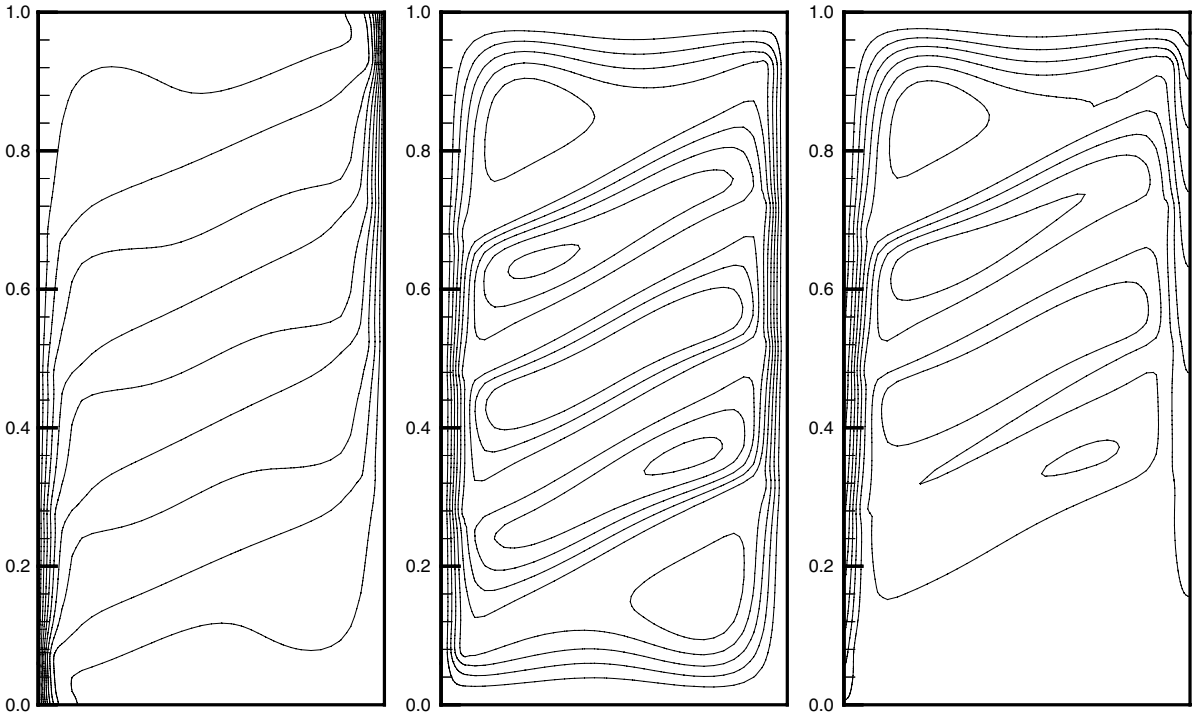

Fig. 8. Results for $\theta = 30°$, $R_c = 1$, $L_* = 0.5$ and $Ra = 10^7$ ($\Delta T_* = 0.10$, $\Delta\psi_* = 2.89$, $\Delta H_* = 1.14$). Base legend as for Fig. 3.

3.2. Temperature field, flow structure, and heat transfer visualization

Throughout this section, starting with Fig. 2, the results are presented in terms of dimensionless isotherms, streamlines and heatlines, from left to right. Fig. 2 corresponds to the main enclosure without shutters, and with $L_* = 0.2$ and $Ra = 10^7$. The isotherms show the usual behavior for high Rayleigh number natural convection in enclosures. Streamlines indicate a single clockwise vortex centered in the main enclosure, with intense upward and downward flows adjacent to the left hot wall and to the right cold wall, respectively. Heatlines show heat flow leaving the hot wall mainly on its lower half, and reaching the cold wall mainly on its upper half. This behavior is commonly encountered in confined high Rayleigh number natural convection.

Results for the enclosure with shutters, and for $\theta = 0°$, $R_c = 1$, $L_* = 0.2$ and $Ra = 10^7$ are presented in Fig. 3. In this case, as $\theta = 0°$, the gap between the vertical walls and the shutters takes its minimum value $\delta_* = 0.001$—for such a small value the partial enclosure's behavior is similar to that for a closed square enclosure with dimensionless height equal to $L_* = 0.2$. The streamlines corroborate this finding as they resemble those corresponding to a vertical stack of closed square enclosures. The Rayleigh number based on the total height H is $Ra = 10^7$, therefore the Rayleigh number for an individual enclosure is approximately (neglecting the shutters' thickness) $Ra_1 \approx Ra(1/5)^3 = 8 \times 10^4$. Heat exchanged between contiguous enclosures, is $(\partial T_*/\partial n_*)_f = (\partial T_*/\partial n_*)_s$ since $R_c = 1$, a condition which can be noted in the isotherms' profile. Heatlines clearly denote that heat leaves uniformly the hot wall through its full height, while the heat reaches the cold vertical wall also uniformly.

The results for $\theta = 30°$ are presented in Fig. 4. The isotherms are nearly horizontal in the region of the shutters, and meandering vertically across the central region of each partial enclosure. The streamlines show a flow structure consisting of clockwise vortices within each partial enclosure, and they are conditioned essentially by the solid walls that contain them. For $\theta = 30°$ the minimum dimensionless gap width is 0.014, that is, 7.0% of the total width, thus allowing fluid flow between adjacent enclosures in the stack, as clearly identified by the streamlines. For this value of the inclination angle, however, the flow in each partial enclosure is primarily

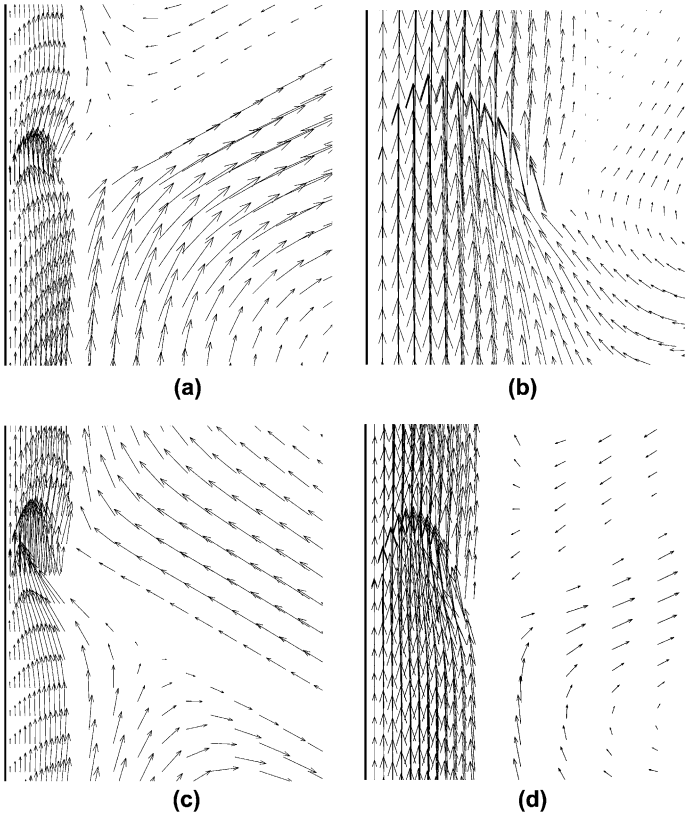

Fig. 9. Dimensionless velocity vectors in the region of the hot-side entering jet of the central partial enclosure for $R_c = 1$ and $Ra = 10^7$, and: (a) $\theta = 30°$ and $L_* = 0.2$; (b) $\theta = 60°$ and $L_* = 0.2$; (c) $\theta = -30°$ and $L_* = 0.2$; and (d) $\theta = 30°$, and $L_* = 0.5$.

controlled by the solid walls of the enclosure and not by the flow occurring through the gap. The influence of the gap over the recirculating flow, for the central partial enclosure, can be evaluated using the ratio between the dimensionless mass flow ratio flowing up through the left-hand middle height of the enclosure, for which $y_* = 0.50$ and $0 \leqslant x_* \leqslant L_*/2$, and the dimensionless mass flow rate flowing towards the right-hand side through the half vertical plane of the enclosure, for which $x_* = L_*/2$ and $0.50 \leqslant y_* \leqslant 0.60$. In this case, the mass flow ratio is of 17.99/15.24 = 1.18, which indicates a minor influence of the gap flow. Heatlines are strongly conditioned by the flow field and, to some extent, by the communicating flow between adjacent enclosures—heat can flow through two adjacent enclosures, when traveling from the hot wall to the cold wall. Values of the heatfunction show that the global heat transfer through the stack decreases as θ increases from $\theta = 0°$ to 30°.

Results corresponding to the same conditions, except for θ, which was taken equal to $\theta = 60°$, are presented in Fig. 5. Strong changes can be observed for the isotherms, which now are very sparse in the interior of each partial enclosure, and of high concentration at the lower half of the hot wall and at the upper half of the cold wall. High concentration of isotherms indicate high thermal gradients and high local heat fluxes, a physical trend which is also given by the heatlines. Values of the heatfunction clearly indicate that the overall heat flow through the stack is higher for $\theta = 60°$ than for $\theta = 30°$. For $\theta = 60°$, the dimensionless minimum gap width is 0.05, that is, 25.0% of the total width, thus allowing intense fluid flow between adjacent partial enclosures. This is shown by the streamlines, which reveal a main clockwise fluid loop through the gaps, and only a low flow rate within each partial enclosure. Values of the streamfunction indicate the fluid flow intensifies as θ increases. The influence of the gap is evaluated in a similar way as before, and the corresponding dimensionless mass flow rate ratio is 30.27/3.85 = 7.86, which means the fluid flow is mainly conditioned by the flow through the gaps. Similarly, the heat transfer is also controlled by the flow through the gaps.

Results for $\theta = 30°$, $R_c = 100$, $L_* = 0.2$ and $Ra = 10^7$ are presented in Fig. 6. When they are compared with the results presented in Fig. 4, for $R_c = 1$, it is apparent the higher thermal conductivity of the shutters yield only minor changes on the isotherms and on the heatlines. Values of the streamfunction indicate the flow is only slightly more intense for $R_c = 1$ than for $R_c = 100$, while

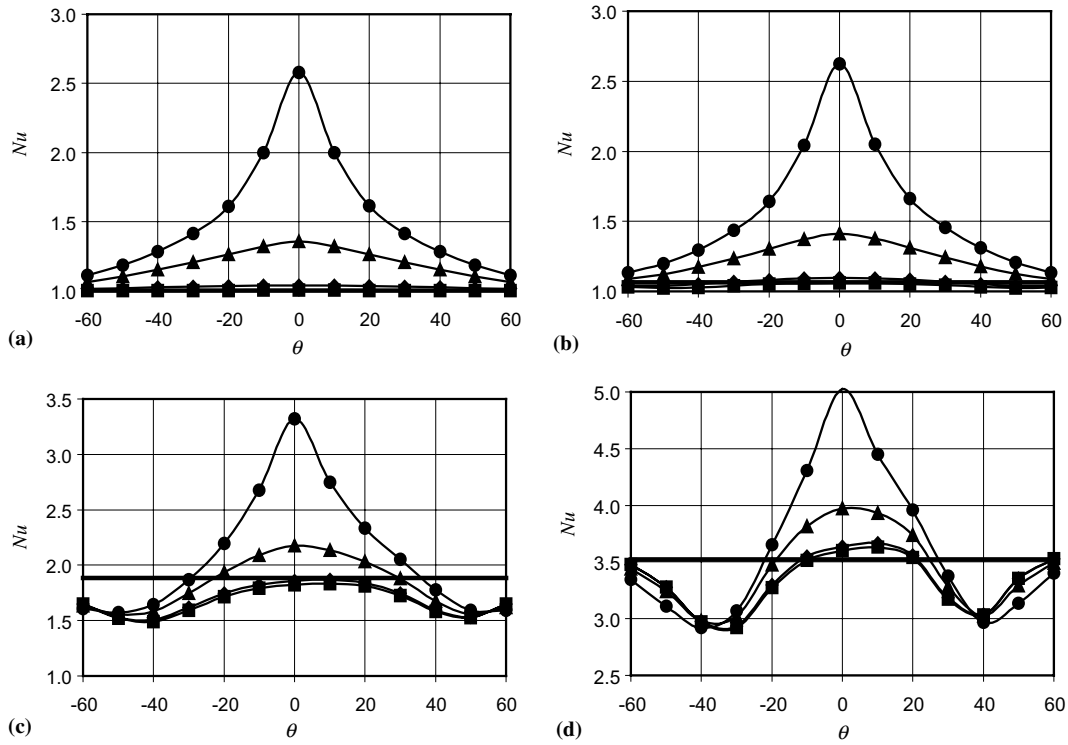

Fig. 10. Global Nusselt number dependency on the inclination angle θ and on the thermal conductivity ratio R_c for the stack with $L_* = 0.2$ and: (a) $Ra = 10^4$ ($Nu_0 = 1.00$); (b) $Ra = 10^5$ ($Nu_0 = 1.07$); (c) $Ra = 10^6$ ($Nu_0 = 1.88$); (d) $Ra = 10^7$ ($Nu_0 = 3.52$). ((—■—) $R_c = 1$, (—◆—) $R_c = 10$, (—▲—) $R_c = 100$, (—●—) $R_c = 1000$).

the values of the heatfunction show the overall heat transfer is only slightly higher for $R_c = 100$ than for $R_c = 1$. These differences are only minor because the shutters considered are very thin; if the shutters were thicker, the influence of the value of R_c would have been more important. For the case presented in Fig. 6, the quantification of the influence of the gap over the recirculating flow yields a small value for the mass flow rate ratio (17.86/15.19 = 1.18).

Negative inclination angles can be equally obtained with the proposed arrangement, and the results for $\theta = -30°$, $R_c = 1$, $L_* = 0.2$ and $Ra = 10^7$ are presented in Fig. 7. In this case, the inclination is not favorable to the fluid flow (the inclined walls are not aligned with the natural flow development), thus resulting a reduction in fluid flow and heat transfer for $\theta = -30°$. Differences between the isotherms for $\theta = 30°$ and for $\theta = -30°$ are considerable. For instance, it is clearly noticeable the strong stand toward the right-hand side of the enclosure of the isotherms for $\theta = -30°$. Close examination of the streamfunction values indicates the fluid flow rate is lower for $\theta = -30°$ than for $\theta = 30°$. Values of the heatfunction also indicate the overall heat transfer through the stack is lower for $\theta = -30°$ than for $\theta = 30°$. The influence of the gap over the recirculating flow gives, in this case, the mass flow rate ratio 13.16/9.43 = 1.40.

Results for $\theta = 30°$, $R_c = 1$, $L_* = 0.5$ and $Ra = 10^7$ are presented in Fig. 8. The isotherms have their highest concentration at the lower half of the hot wall and at the upper half of the cold wall, the heat flow is in agreement with this distribution as clearly indicated by the heatlines. In this case, the minimum dimensionless gap width is 0.034, that is, 6.8% of the total width. This gap magnitude does allow significant fluid flow between contiguous partial enclosures, as indicated by the streamlines. Analysis of the values of the streamfunction show fluid flow is considerably more intense for $L_* = 0.5$ than for $L_* = 0.2$ (Fig. 4). Values of the heatfunction also indicate that the global heat transfer is less intense for $L_* = 0.2$ than for $L_* = 0.5$.

The shutters with an inclination angle $\theta \neq 0$ yield an interesting complex flow occurring at the edge of the shutters, where an accelerating 'jet' penetrates the edges of an essentially recirculating flow. The flow structure in the region of the hot-side entering jet of the central partial enclosure is presented in Fig. 9a–c for some of the foregoing considered situations.

For all the cases analyzed, the isotherms and the streamlines for the central partial enclosure in the stack

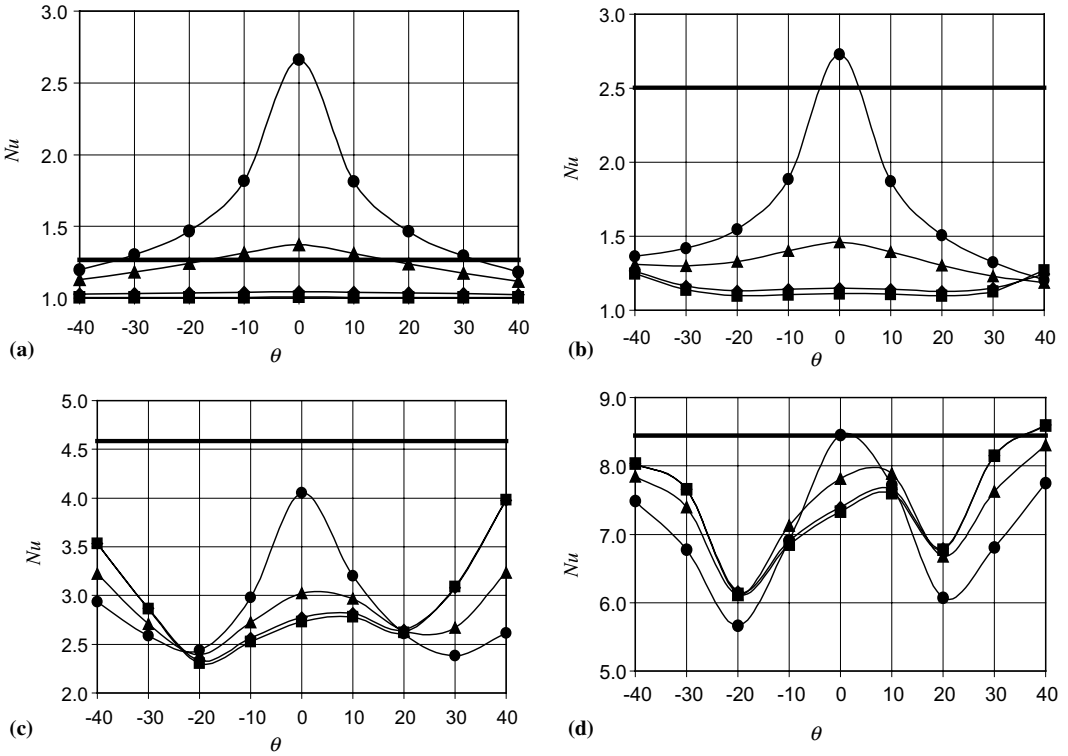

Fig. 11. Nusselt number results for the stack with $L_* = 0.5$ and: (a) $Ra = 10^4$ ($Nu_0 = 1.27$); (b) $Ra = 10^5$ ($Nu_0 = 2.51$); (c) $Ra = 10^6$ ($Nu_0 = 4.59$); (d) $Ra = 10^7$ ($Nu_0 = 8.45$). Remaining legend as for Fig. 10.

clearly show that this individual enclosure suffers only small influences from the top and bottom conditions of the global stack, and such an enclosure can be taken as representative of the global vertical stack, composed of many of such partial enclosures, being this enclosure nearly under vertical cyclic boundary conditions. Analyses are conducted for the heat transfer performance of the global stack and of the particular enclosure representative of the stack, and, in this case, the cyclic boundary conditions in the vertical direction are used.

3.3. Heat transfer analysis

The heat transfer analysis is conducted by analyzing the dependence of the overall Nusselt number on the inclination angle, thermal conductivity ratio and Rayleigh number for stacks with various values of L_*. It should be noted that the Nusselt number definition is made taken the pure conduction situation as reference, which is $\dot{Q}' = k_f(T_H - T_C)/(L/H) = (1/L_*)k_f(T_H - T_C)$, and that the true global heat transfer, by unit depth, is $\dot{Q}' = (Nu/L_*)k_f(T_H - T_C)$. Thus, for heat transfer comparisons it should be used the ratio (Nu/L_*) and not the Nusselt number, Nu, only.

Fig. 10a–d present the overall Nusselt number for a stack with $L_* = 0.2$. For comparison purposes, the Nusselt number corresponding to the global enclosure with no shutters, Nu_0, with the same dimensionless parameters L_* and Ra, is also presented. Results show that the maximum heat transfer is obtained for an inclination angle close to zero, and higher values of Ra yield higher values of Nu. This effect is more pronounced for small inclination angles, for which shutters of higher thermal conductivity nearly set a conductive mode for heat transfer between the heat and cold walls.

Another important aspect to refer is the nearly symmetric behavior around $\theta = 0$ of the Nusselt number with the inclination angle. For small values of the Rayleigh number ($Ra = 10^4$, 10^5), the buoyancy induced flow is small, and the heat transfer occurs primarily by conduction through the nearly stagnant fluid. As $|\theta|$ increases, so increases the gap width and decreases the influence of the shutters, and the overall Nusselt number approaches the value corresponding to that for the enclosure with no shutters. As the Rayleigh number increases so increases the buoyancy induced flow, advective transport becomes more important, and the overall Nusselt number increases. For small absolute

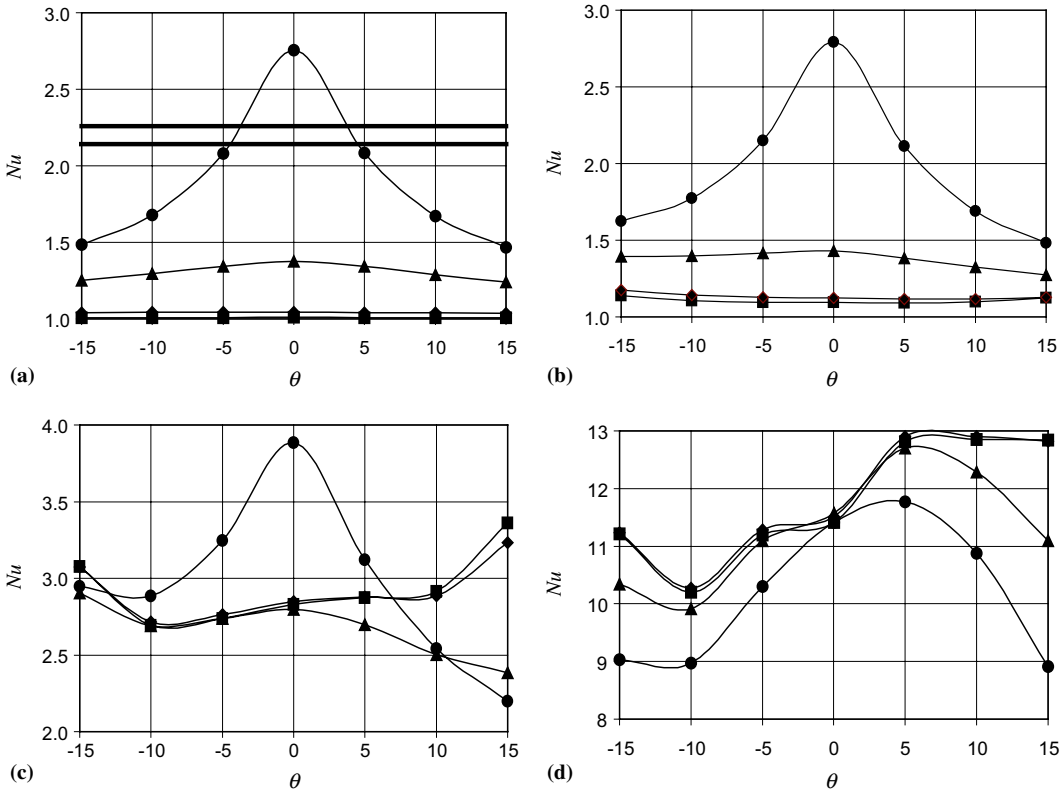

Fig. 12. Nusselt number results for the stack with $L_* = 1.0$ and: (a) $Ra = 10^4$ ($Nu_0 = 2.26$); (b) $Ra = 10^5$ ($Nu_0 = 4.55$); (c) $Ra = 10^6$ ($Nu_0 = 8.89$); and (d) $Ra = 10^7$ ($Nu_0 = 16.83$). Remaining legend as for Fig. 10.

values of the inclination angle, the stack approaches a vertical series of almost closed enclosures, the overall Nusselt number being the summation of each individual enclosure's contribution. For high values of the inclination angle, the gap width becomes high and the fluid flow and heat transfer adjacent to the vertical walls approaches the condition of the overall enclosure with no shutters. Thus, the overall Nusselt number for high values of the inclination angle is close to that for the overall enclosure with no shutters, a behavior, which can be observed in Fig. 10c and d. For intermediate values of the inclination angle, the shutters together with the vertical walls act like nozzles for the fluid flow, thus decreasing its intensity, and its advection importance. This yields a minimum for the overall heat transfer rate, which corresponds approximately to $\theta = -40°$ or $\theta = 50°$ for $Ra = 10^6$, and nearly to $\theta = -35°$ or $40°$ for $Ra = 10^7$. For high Rayleigh numbers, however, for moderate to high values of the inclination angle, advection is dominant, and the influence of the thermal conductivity of the shutters is of minor importance. For engineering purposes, if the objective is to increase the heat transfer, then shutters of high thermal conductivity should be used, with zero inclination angle. If heat transfer is to be reduced, for high Rayleigh numbers, inclination angles for the shutters should be selected accordingly, and the shutters' thermal conductivity is not of particular importance.

Many of the explanations and interpretations given for Fig. 10a–d are also valid for the figures that follow, and they will not be repeated.

The Nusselt numbers for the stack with $L_* = 0.5$ are presented in Fig. 11a–d. The variation of θ was restricted due to geometrical arguments. These results, when compared with those for the enclosure with $L_* = 0.2$ (Fig. 10a–d), yield the finding that a stack with higher aspect ratio ($L_* = 0.5$) leads to higher heat transfer rates than those for the stack with $L_* = 0.2$. A general conclusion that can be taken from Fig. 11a–d is that, with the shutters, considerable reduction can be obtained on heat transfer, reductions that can be achieved even for low Rayleigh number values. The decrease that can be obtained on the overall heat transfer rate is, however, more pronounced for high Rayleigh numbers. The optimum reported reduction corresponds to $\theta = -20°$ or $20°$ for $Ra = 10^6$ and for $Ra = 10^7$. For $Ra = 10^7$, and for moderate to high inclination angles, lower heat transfer rates are obtained with shutters of high thermal conductivity. This is due to the relative increase of the time for heat exchange between the hot and cold streams on both sides of the shutters, due to the increase of the shutters' length. This gives rise to lower heat extraction from the

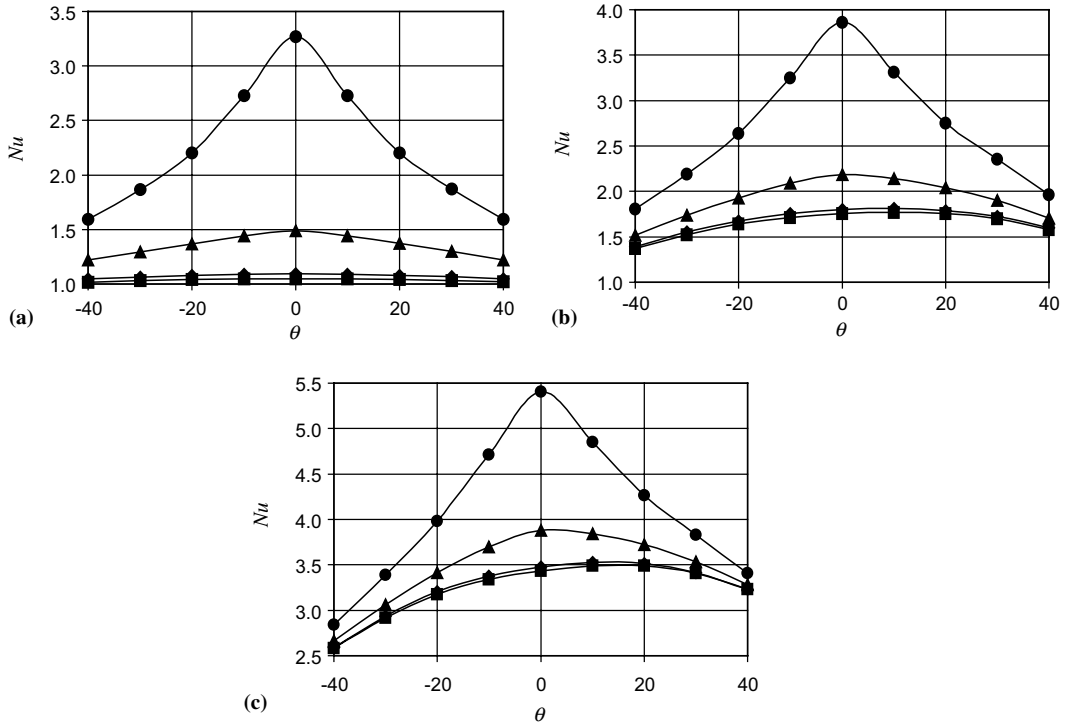

Fig. 13. Nusselt number results for the individual enclosure subject to vertical periodic boundary conditions, $L_* = 0.2$ and: (a) $Ra = 10^5$; (b) $Ra = 10^6$; and (c) $Ra = 10^7$. ((—■—) $R_c = 1$, (—◆—) $R_c = 10$, (—▲—) $R_c = 100$, (—●—) $R_c = 1000$).

hot wall, and consequent lower heat rejection on the cold wall. Following this argument, thinner shutters lead to greatest overall heat transfer reductions. Increases on the overall Nusselt number are obtained for reasonably low Rayleigh numbers only, a conduction dominated situation where the thermal conductivity of the shutters is very important. It should be also noted the loss of symmetry on the results in Fig. 11c and d, relative to $\theta = 0$. The partial enclosures are parallelogrammic in nature, and it is well-known that, for moderate or high L_* ratio, a positive inclination angle θ gives rise to higher heat transfer rates than the corresponding negative inclination angle $-\theta$ (thermal diode effect of the parallelogrammic enclosures) [18,21].

Results of the overall Nusselt number for the stack with $L_* = 1.0$ are presented in Fig. 12a–d. For $Ra > 10^4$, the overall Nusselt number for the enclosure with no shutters is considerably higher than the overall Nusselt number for the enclosure with shutters, which is not shown in the figures, but its value is indicated in the caption. The thermal conductivity of the shutters is more relevant for inclination angles close to zero, exception made for high Rayleigh number situations, for which the shutters' thermal conductivity is also relevant for high values of the inclination angle. For $Ra = 10^6$ and $\theta = 15°$ lower heat transfer rates are obtained for higher thermal conductivity of the shutters. For $Ra = 10^7$ strong changes do occur. Lower heat transfer rates are obtained, for any inclination angle, for the highest thermal conductivity of the shutters. The time for heat exchange between the hot and cold streams on both sides of the shutters increases as increases the shutters' length, and lower overall heat transfer results. Therefore, the importance of the thermal conductivity of the shutters remains even for high values of the inclination angle. In this case, the thickness of the momentum and temperature boundary layers is mainly conditioned by the distance between the shutters and not by the gap width, and the Nusselt numbers for high values of θ are always lower than the Nusselt numbers for the enclosure with no shutters. Significant in Fig. 12d is the non-symmetry around $\theta = 0$, the heat transfer rate being higher for positive values of θ than for negative values of θ, except for shutters with high thermal conductivity.

3.4. Heat transfer analysis using vertical cyclic boundary conditions

As referred before, for a vertical stack with high aspect ratio, composed of a large number of shutters, the best way to evaluate its thermal performance is from

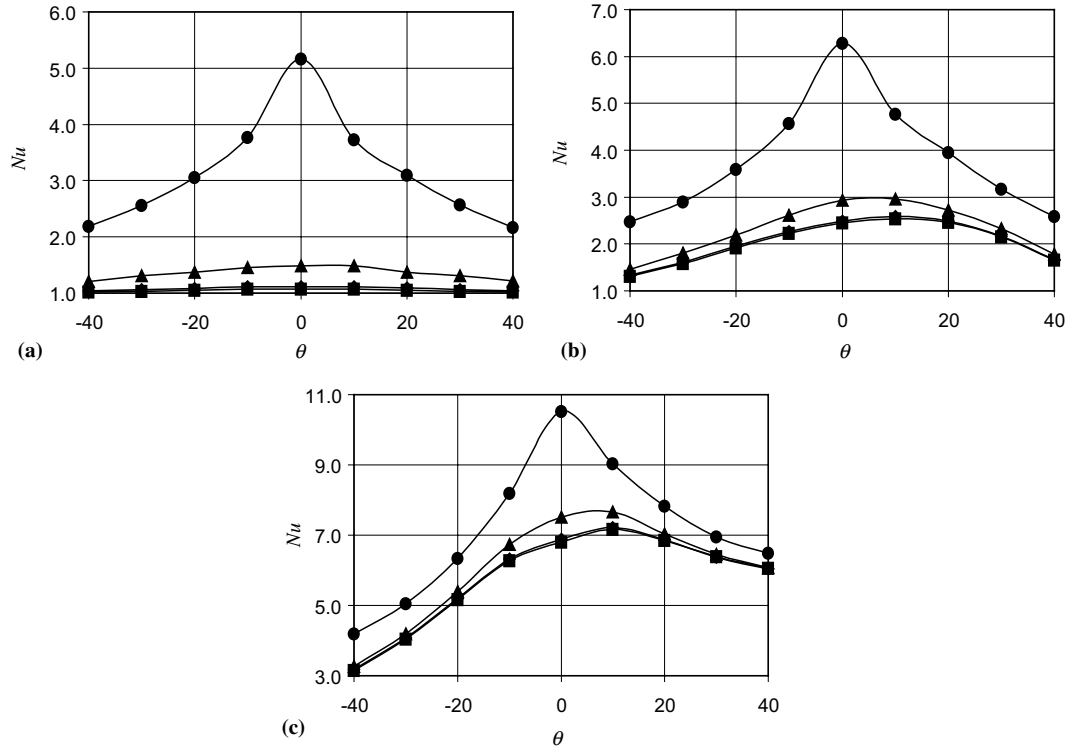

Fig. 14. Nusselt number results for the enclosure with $L_* = 0.5$ and: (a) $Ra = 10^5$; (b) $Ra = 10^6$; and (c) $Ra = 10^7$. Remaining legend as for Fig. 13.

the perspective of a single partial enclosure subject to vertical cyclic boundary conditions [29]. Such single enclosure is under mixed convection conditions, as it is under the influence of the inlet jets, coming from the neighboring partial enclosures, and under natural convection influence of the thermal buoyancy force. It should be stressed out that the results were obtained for selected Rayleigh numbers based on the total height of the full stack, the Rayleigh number for an individual partial enclosure being $Ra_1 \approx Ra(1/5)^3 = Ra/125$.

It should be mentioned that numerical convergence problems, possibly due to numerical instabilities induced by the cyclic boundary conditions, were experienced for high values of $|\theta|$ and, in some cases, for $L_* = 1.0$. The reason for this particular behavior, despite extensive numerical testing, was left unanswered.

Results for the enclosure with $L_* = 0.2$ are presented in Fig. 13a–c, and when compared with the corresponding results for the stack (Fig. 10b–d), yield the following observations: (i) the Nusselt number results for the enclosure under the cyclic conditions are slightly higher than those for the stack, and (ii) the general dependence of the Nusselt number upon θ and R_c is similar in both cases. It is also observed that, for $Ra = 10^7$, the cyclic results do not exhibit a minimum Nusselt number for the analyzed range for which $|\theta| \leqslant 40°$, a finding which should be taken into account when designing high stacks, with many shutters.

Results for the Nusselt number with the enclosure with $L_* = 0.5$ are presented in Fig. 14a–c. The main conclusions extracted from these figures are similar to those extracted from the analysis of the results for the enclosure with $L_* = 0.2$.

4. Conclusions

Parallelogrammic enclosures, when considered individually, present a phenomenological feature usually known as thermal diode effect. This effect reflects on the thermal performance of the enclosure, yielding either heat transfer enhancement or reduction. When they are assembled in a vertical stack of thermally communicating enclosures, they continue to preserve very interesting thermal characteristics that should be explored and incorporated in heat transfer/thermal insulation products.

In this work it is proposed an arrangement for a vertical stack of enclosures with the possibility of variable geometry (inclination angle). In this way, the internal geometry of the stack can be changed depending of the thermal boundary conditions, thus allowing the best thermal performance required for a particular stack. Such an arrangement leads to a vertical stack of parallelogrammic partial enclosures, which are in communication with the neighboring partial enclosures through the flow exchange and through the heat exchange occurring across the shutters of finite thermal conductivity. From the heat and mass transfer viewpoints, it is a challenging problem, with complex flow structures appearing in the neighboring of the narrow region between the vertical walls and the shutters' edges, where a recirculating flow is combined with a natural convection generated jet flow.

The physical model clearly identifies the governing parameters, and the results obtained clearly identify and clarify the features of the proposed stack arrangement. Adequately used, it can lead to walls of variable thermal performance, which can be changed, or even optimized, depending on the imposed thermal loads and temperature conditions. Results also show how the thermal performance of an enclosure without shutters is changed by the shutters' introduction, and how important is the thermal conductivity of the shutters on the resulting global thermal performance.

For a high stack, composed by many partial enclosures, its thermal performance can be evaluated from the results obtained for a single partial enclosure subject to vertical cyclic boundary conditions. Preliminary results were obtained following this procedure, which seems to be a 'natural' way of solution in engineering situations.

Acknowledgments

This research work received partial funding from TEMA (Centre for Mechanical Engineering and Automation) under the Foundation for Science and Technology—FCT (Portugal), R&D Units' Program, and Natural Science and Engineering Research Council of Canada (NSERC) Discovery Grant, RGPIN 1398-98 (ACMS).

References

[1] A. Bejan, Convection Heat Transfer, second ed., Wiley, New York, 1995.
[2] S. Ostrach, Natural convection in enclosures, ASME J. Heat Transfer 110 (1988) 1175–1189.
[3] R. Scozia, R.L. Frederick, Natural convection in slender cavities with multiple fins attached to an active wall, Numer. Heat Transfer: Part A 20 (1991) 127–158.
[4] R.L. Frederick, A. Valencia, Natural convection in central microcavities of vertical, finned enclosures of very high aspect ratio, Int. J. Heat Fluid Flow 16 (1995) 114–124.
[5] E.K. Lakhal, M. Hasnaoui, E. Bilgen, P. Vasseur, Natural convection in inclined rectangular enclosures with perfectly conducting fins attached on the heated wall, Int. J. Heat Mass Transfer 32 (1997) 365–373.

[6] N. Yucel, H. Turkoglu, Numerical analysis of laminar natural convection in enclosures with fins attached to an active wall, Int. J. Heat Mass Transfer 33 (1998) 307–314.
[7] R.L. Frederick, A. Valencia, Heat transfer in a square cavity with a conducting partition on its hot wall, Int. Commun. Heat Mass Transfer 16 (1989) 347–354.
[8] E. Zimmerman, S. Acharya, Free convection heat transfer in a partially divided vertical enclosure with conducting end walls, Int. J. Heat Mass Transfer 30 (1987) 319–331.
[9] T. Nishimura, Natural convection in horizontal enclosures with multiple partitions, Int. J. Heat Mass Transfer 32 (9) (1989) 1641–1647.
[10] K.M. Kelkar, S.V. Patankar, Numerical prediction of natural convection in square partitioned enclosures, Numer. Heat Transfer 17 (1990) 269–285.
[11] E. Bilgen, Natural convection in enclosures with partial partitions, Renew. Energy 26 (2002) 257–270.
[12] K. Bae, H. Chung, H. Jeong, Convective heat transfer in ventilated space with various partitions, KSME Int. J. 16 (5) (2002) 676–682.
[13] R.D. Flack, T.T. Konopnicki, J.H. Rooke, The measurement of natural convective heat transfer in triangular enclosures, ASME J. Heat Transfer 101 (1979) 648–654.
[14] D. Poulikakos, A. Bejan, Natural convection experiments in a triangular enclosure, ASME J. Heat Transfer 105 (1983) 652–655.
[15] H. Salmun, Convection patterns in a triangular domain, Int. J. Heat Mass Transfer 38 (2) (1995) 351–362.
[16] F. Moukalled, S. Acharya, Buoyancy induced heat transfer in partially divided trapezoidal cavities, Numer. Heat Transfer 32 (8) (1998) 787–810.
[17] F. Moukalled, S. Acharya, Natural convection in trapezoidal cavities with baffles mounted to their upper inclined surfaces, Numer. Heat Transfer A 37 (2000) 545–565.
[18] K.C. Chung, L.M. Trefethen, Natural convection in a vertical stack of inclined parallelogrammic cavities, Int. J. Heat Mass Transfer 25 (2) (1982) 277–284.
[19] N. Seki, S. Fokosako, A. Yamagushi, An experimental study of free convective heat transfer in a parallelogrammic enclosure, ASME J. Heat Transfer 105 (1983) 433–439.
[20] J.M. Hyun, B.S. Choi, Transient natural convection in a parallelogram-shaped enclosure, Int. J. Heat Fluid Flow 11 (2) (1990) 129–134.
[21] V.A.F. Costa, A.R. Figueiredo, L.A. Oliveira, Natural convection in parallelogramic cavities, in: Proceedings of the I Congreso Iberoamericano de Ingeniería Mecánica, E.T.S. Ingenieros Industriales, Madrid, vol. 2, 1993, pp. 255–260 (in Portuguese).
[22] M.-R. Zugari, J.-J. Vullierme, Étude numérique du transfert de chaleur dans une cavité de forme parallélogrammatique et inclinée, à parois pasives minces, Comptes Rendues à L'Academie des Sciences de Paris, Tome 319, Série II, 1994, pp. 1157–1163.
[23] K.D. Aldridge, H. Yao, Flow features of natural convection in a parallelogrammic enclosure, Int. Commun. Heat Mass Transfer 28 (7) (2001) 923–931.
[24] Z. Zang, A. Bejan, J.L. Lage, Natural convection in a vertical enclosure with internal permeable screen, ASME J. Heat Transfer 113 (1991) 377–383.
[25] J. Phillips, P.H. Oosthuizen, D. Naylor, S.J. Harrison, Numerical study of convective and radiative heat transfer from a window glazing with a venetian blind, HVAC&R Res. 7 (4) (2001) 383–402.
[26] H. Shahid, D. Naylor, Thermal simulations of a fenestration with horizontal venetian blind, in: A.A. Mohamad (Ed.), in: Proceedings of the Third International Conference on Computational Heat and Mass Transfer, Banff, Canada, 2003, pp. 727–736.
[27] V.A.F. Costa, Unification of the streamline, heatline and massline methods for the visualization of two-dimensional transport phenomena, Int. J. Heat Mass Transfer 42 (1) (1999) 27–33.
[28] V.A.F. Costa, L.A. Oliveira, A.R. Figueiredo, A control volume based finite element method for three-dimensional incompressible turbulent fluid flow, heat transfer, and related phenomena, Int. J. Numer. Methods Fluids 21 (7) (1995) 591–613.
[29] S.V. Patankar, C.H. Liu, E.M. Sparrow, Fully developed flow and heat transfer in ducts having streamwise-periodic variations of cross-sectional area, ASME J. Heat Transfer 99 (1977) 180–186.